Journal of Applied Sciences

ISSN 1812-5654

science alert

ANSInet
an open access publisher
http://ansinet.com

Journal of Applied Sciences 8 (10): 1798-1811, 2008
ISSN 1812-5654

Transient Response of a Spiral Fin with its Base Subjected to the Variation of Heat Flux

[1]J.S. Wang, [2]W.J. Luo and [2]S.P. Hsu
[1]Department of Power Mechanical Engineering, National Taitung College, Taitung, Taiwan
[2]Department of Refrigeration, Air-Conditioning and Energy Engineering,
National Chin-Yi University of Technology, Taiping City,
Taichung County 411, Taiwan

Abstract: The problem of transient response of a spiral fin, with its end insulated, is analyzed with the base end subjected to a variation of fluid temperature. The method of Laplace transforms and with a technique derived by the Keller and Keller, of which has an exponential like form, is applied to study the transient response. Both of a unit step change and a sinusoidal temperature change are analyzed. Moreover, the results of the temperature distribution and the heat flux at the base of the fin are obtained. Solutions are developed for both small and large values of time. Typical results are presented in both tables and graphs. Comparisons are made and the results show a good agreement in the physical circumstance.

Key words: Laplace transforms, transient response, heat transfer

INTRODUCTION

The problem of response in fins has been of much interest for many researchers and engineers due to its magnificently industrial applications. The use of Fins to enhance the heat dissipation from a hot surface is very extensive in many areas of engineering applications. Besides the traditional applications, such as power generator, plants and vehicles, fines are also used in heat removal devices foe electronic components. Park *et al.* (2007) used the pin-fin type heat sinks for different fin shapes to enhance the heat transfer of a heat sink and the optimum values of the design variables such as fin height, fin width or fin diameter and fan-to-heat sink distance at the junction of a heat sink and a heat source are investigated. T'joen *et al.* (2007) applied an experimental study to investigate the performance of a fin-and-tube heat exchanger in two different configurations.

In a conventional heat exchanger heat is transferred from one fluid to another through a metallic wall. The rate of heat transfer is directly proportional to the extent of the wall surface, the heat transfer coefficient and to the temperature difference between one fluid and the adjacent surface. It might be expected that the rate of heat transfer per unit of the base surface area would increase in direct proportion. However, the average surface temperature of the fins tends to decrease approaching the temperature of the surrounding fluid so the effective temperature difference is decreased and the net increase of heat transfer would not be in direct proportion to the increase of the surface area and may be considerably less than that would be anticipated on the basis of the increase of surface area alone. The performance of fin under steady state conditions has been studied in considerable detail but the transient response of such surfaces to changes in either base temperature or base heat flux has not received much attention. Both of one-dimensional and two-dimensional circular fin have been studied broadly. Chu *et al.* (1982, 1983a, b) has applied the Fourier series inversion technique to determine the transient response of two-dimensional straight fins and circular fins, one-dimensional annular fin and the composite straight fins. His results showed a good agreement in the physical circumstances. The transient temperature response of the annular fins, a special case (pitch equal zero) for the spiral fin, was well studied. Cheng *et al.* (1994, 1998) studied the transient response of annular fins of various shapes subjected to constant base heat fluxes. In their work, the inverse method was applied. Yu and Chao-Kuang Chen (1999) applied the Taylor transformation to the transient temperature response of annular fin. When the end of the fin is not insulated, Harper and Brown (1992) have shown that, under certain circumstances, an equivalent fin with end insulated can be obtained by suitably increasing its

Corresponding Author: Win-Jet Luo, Department of Refrigeration, Air-Conditioning and Energy Engineering, National Chin-Yi University of Technology, Taiping City, Taichung County 411, Taiwan
Tel: 886-6-23924505/8255 Fax: 886-6-23932758

length. It is also assumed that one-dimensional analysis is valid. One-dimensional analysis has been shown to be valid under steady state conditions for small Biot number by Crank and Parker (1996). Performance and optimum dimensions of longitudinal and annual fins and spines with a temperature-dependent heat transfer coefficient have been presented by Laor and Kalman (1996). In this study, considered the heat transfer coefficient as a power function of temperature and used exponent values in the power function that represent different heat transfer mechanisms such as free convection, fully developed boiling and radiation. The optimum dimensions of circular fins with variable profile and temperature-dependent thermal conductivity have been obtained by Zubair *et al.* (1996). Campo and Stuffle (1996) presented a simple and compact form correlation that facilitates a rapid determination of fin efficiency and tip temperature in terms of fin controlling parameters for annular fins of constant thickness. Mokheimer (2002) investigated the performance of annular fins of different profiles subject to locally variable heat transfer coefficient. The performance of the fin expressed in terms of fin efficiency as a function of the ambient and fin geometry parameters has been presented in the literature in the form of fin-efficiency curves for different type of fins.

Because fins are frequently used under unsteady conditions, it is worth studying the transient behavior of fins with time-dependent boundary conditions. Otherwise, due to the particular geometry of the spiral fin, the contact surface area of the fin is lager than that of annual fin at the same length. From the through literature survey mentioned above, the effect of temperature-dependent heat transfer coefficient on the fin efficiency of spiral fins has not been investigated. The aim of the present article is to investigate such effects. This type of study would be of direct use by the heat transfer equipment designers and rating engineers. In this study, the solutions of transient response of straight fins are obtained by Laplace transforms that is easy to calculate rapidly convergent approximate solutions for small value of time. After using the Laplace transforms to the differential equation for the temperature of the spiral fin, we can obtain a linear set of second order ordinary differential equation which can be evaluated by employing Keller and Keller's method (Keller and Keller, 1962; Luo and Yang, 2007; Shih *et al.*, 2008). Solutions of the approximately exponential functions were proposed for the partial differential equation in their papers. This is a novel method in solving the nonlinear parabolic second order differential equation. Therefore, through the combination of Laplace transforms and the method derived by Keller and Keller (1962), we evaluate the transient response of a spiral fin with the base subjected to a variation of fluid temperature.

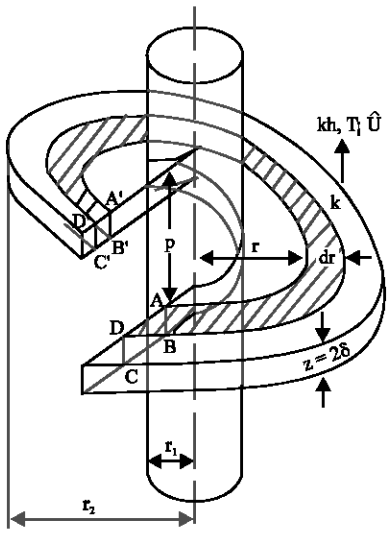

Fig. 1: The physical model of a spiral fin

Analysis: The physical system consisting of a spiral fin of uniform thickness 2δ, inner radius r_1, outer radius r_2, pitch P and thermal conductivity k is shown in Fig. 1. The end of the fin, i.e., $r = r_2$, is assumed to be perfectly insulated. It is also assumed that one-dimensional analysis is valid. Initially, the fin is in thermal equilibrium with the surrounding fluid temperature T_∞. At time t = 0, the base temperature is suddenly raised to T_f or subjected to heat flux q_0* and from then on, the spiral fin dissipated heat by convection to the environment through a convective heat transfer coefficient h, h_f and the properties k, ρ, c of the material of the fin are all assumed to be constant. At the other boundary condition, i.e., at $r = r_1$, the convective boundary condition by ignoring the thermal resistance and capacity of the material in inner wall tube is assumed.

From the conservation of energy, we can get the differential equation of the temperature of spiral fin from the balance of energy, as following:

$$\frac{\partial}{\partial r}\left\{\sqrt{\left(\frac{P}{2\pi}\right)^2+r^2}\,\frac{\partial T}{\partial r}\right\}-\frac{h}{k\delta}\sqrt{\left(\frac{P}{2\pi}\right)^2+r^2}\,[T-T_\infty]=\frac{1}{\alpha}\sqrt{\left(\frac{P}{2\pi}\right)^2+r^2}\,\frac{\partial T}{\partial t},\quad t>0,\ r_1<r<r_2 \tag{1}$$

where, $\alpha = k/\rho c$ is the thermal diffusivity and Biot number is $B_i = h_f r_1/k_f$.

After introducing the non-dimensional variables,

$$\xi=\frac{r}{r_1},\ \phi=\frac{T-T_\infty}{T_f-T_\infty},\ \alpha=\frac{\alpha t}{r_1^2},\ P_1=\frac{P}{2\pi r_1},\ R=\frac{r_2}{r_1},\ N^2=\frac{hr_1^2}{k\delta}$$

The dimensionless governing equation is:

$$\frac{\partial}{\partial\xi}\left\{\sqrt{P_i^2+\xi^2}\,\frac{\partial\phi}{\partial\xi}\right\}-N^2\sqrt{P_i^2+\xi^2}\,\phi=\sqrt{P_i^2+\xi^2}\,\frac{\partial\phi}{\partial\tau},\quad \tau>0,\ 1<\xi<R \tag{2}$$

The analysis of the transient response of spiral fin subjected to a variation of fluid temperature will be studied in the two following cases.

Case 1: A unit step change in base fluid temperature: For the case 1, the heat transfer of the fin which base is subjected to a constant temperature is investigated. The ambient temperature is kept constant and no heat sources or sinks are present. The dimensionless initial and boundaries can be defined as:

$$\phi(\xi,0)=0,\quad 1<\xi<R \tag{3}$$

$$-\frac{\partial\phi}{\partial\xi}+B_i\phi=B_i,\quad \xi=1,\ \tau>0 \tag{4}$$

$$-\frac{\partial\phi}{\partial\xi}(R,\tau)=0,\quad \tau>0 \tag{5}$$

where, B_i is the Biot number, $B_i = h_f r_1/k_f$. Taking the Laplace transformation with respect to τ for Eq. 2 and using the initial condition (3), we can express the differential equation as:

$$\frac{d}{d\xi}\left\{\sqrt{P_i^2+\xi^2}\,\frac{d\bar{\phi}}{d\xi}\right\}-\left\{\sqrt{P_i^2+\xi^2}\left[N^2+s\right]\right\}\bar{\phi}=0 \tag{6}$$

where, s is the transformed variable. After neglecting the integrals in the coefficient of exponentials, the Keller and Keller's solution of Eq. 6 is:

$$\bar{\phi}(\xi,s)=D_2\left\{-\left[N^2+s\right]\left[P_i^2+\xi^2\right]\right\}^{-1/4}\cdot\cosh\left[\sqrt{N^2+s}\,(R-\xi)\right] \tag{7}$$

where, D_2 is a constant to be determined by the boundary condition (4). After employing Laplace transformation, the boundary condition (4) can be express as:

$$-\frac{d\bar{\phi}}{d\xi}+B_i\bar{\phi}=\frac{B_i}{s},\quad \xi=1 \tag{8}$$

Substituting Eq. 7 into Eq. 8, the constant D_2 can be express as:

$$D_2=\frac{2B_i\left[-\left(N^2+s\right)\right]^{1/4}\left[P_i^2+1\right]^{3/2}}{\left\{2\left[P_i^2+1\right]^{5/4}\cdot\sqrt{N^2+s}\cdot s\cdot\sinh\left[\sqrt{N^2+s}\,(R-1)\right]+s\left[P_i^2+1\right]^{1/4}\cdot\cosh\left[\sqrt{N^2+s}\,(R-1)\right]\left[2B_i\left(P_i^2+1\right)+1\right]\right\}} \tag{9}$$

Thus, Eq. 7 becomes:

$$\bar{\phi}(\xi,s)=\frac{2B_i\left[P_i^2+1\right]^{5/4}}{s\left[P_i^2+\xi^2\right]^{-1/4}}\cdot\frac{\cosh\left[\sqrt{N^2+s}\,(R-\xi)\right]}{\left\{2\left[P_i^2+1\right]\sqrt{N^2+s}\sinh\left[\sqrt{N^2+s}\,(R-1)\right]+\left[2B_i\left(P_i^2+1\right)+1\right]\cdot\cosh\left[\sqrt{N^2+s}\,(R-1)\right]\right\}} \tag{10}$$

Applying the contour integral method, the inverse transform of the temperature distribution is:

$$\phi(\xi,\tau)=\frac{1}{2\pi i}\int_{r-i\infty}^{r+i\infty}\frac{2B_i\left[P_i^2+1\right]^{5/4}e^{z\tau}}{z\left[P_i^2+\xi^2\right]^{1/4}}\cdot\frac{\cosh\left[\sqrt{N^2+z}\,(R-\xi)\right]}{\left\{2\left[P_i^2+1\right]\sqrt{N^2+z}\sinh\left[\sqrt{N^2+z}\,(R-1)\right]+\left[2B_i\left[P_i^2+1\right]+1\right]\cdot\cosh\left[\sqrt{N^2+z}\,(R-1)\right]\right\}}dz$$
$$=R_{es}(0)+\sum_{n=1}^{\infty}R_{es}(Z_{on})\Bigg|_{\left\{2\left[P_i^2+1\right]\sqrt{N^2+z_{on}}\sinh\left[\sqrt{N^2+z_{on}}\,(R-1)\right]+\left[2B_i\left(P_i^2+1\right)+1\right]\cosh\left[\sqrt{N^2+z_{on}}\,(R-1)\right]=0\right\}} \tag{11}$$

Where:

$$R_{es}(0)=\frac{2B_i\left[P_i^2+1\right]^{5/4}}{\left[P_i^2+\xi^2\right]^{1/4}}\cdot\left\{\frac{\cosh\left[N(R-\xi)\right]}{2N\left[P_i^2+1\right]\sinh\left[N(R-1)\right]+\left[2B_i\left(P_i^2+1\right)+1\right]\cdot\cosh\left[N(R-1)\right]}\right\} \tag{12}$$

$$\sum_{n=1}^{\infty}R_{es}(z_{on})=-\frac{4B_i\left[P_i^2+1\right]^{5/4}}{\left[P_i^2+\xi^2\right]^{1/4}}\cdot\sum_{n=1}^{\infty}\frac{e^{-\left[\frac{\lambda_n^2}{(R-1)^2}+N^2\right]\tau}\cos\left[\lambda_n\left(\frac{R-\xi}{R-1}\right)\right]}{\left[\frac{\lambda_n^2}{(R-1)^2}+N^2\right]\left[\sin\lambda_n\right]\left\{\frac{4\left[P_i^2+1\right]^2\lambda_n}{2B_i\left(P_i^2+1\right)+1}+\frac{2\left[P_i^2+1\right](R-1)+2B_i\left[P_i^2+1\right](R-1)^2+(R-1)^2}{\lambda_n}\right\}} \tag{13}$$

The λ_n s in the above equations can be calculated from the following equation:

$$\lambda_n\tan\lambda_n=\frac{(R-1)\left[2B_i\left(P_i^2+1\right)+1\right]}{2\left(P_i^2+1\right)},n=1,2,3,\cdots \tag{14}$$

The temperature distribution $\phi(\xi, \tau)$ is then given by the sum of Eq. 12 and 13 associated with the λ_n's determined by Eq. 14. The temperature distribution valid for small values of time can be obtained by applying the methods of Ozisik (1980). It can be expressed as:

$$\phi(\xi,\tau)=\frac{2B_i\left[P_i^2+1\right]^{5/4}}{\left[P_i^2+\xi^2\right]^{1/4}}\cdot\left\{\frac{\cosh\left[N(R-\xi)\right]}{2N\left[P_i^2+1\right]\sinh\left[N(R-1)\right]+\left[2B_i\left(P_i^2+1\right)+1\right]\cdot\cosh\left[N(R-1)\right]}\right\}$$
$$-\frac{4B_i\left[P_i^2+1\right]^{5/4}}{\left[P_i^2+\xi^2\right]^{1/4}}\cdot\sum_{n=1}^{\infty}\frac{e^{-\left[\frac{\lambda_n^2}{(R-1)^2}+N^2\right]\tau}\cos\left[\lambda_n\left(\frac{R-\xi}{R-1}\right)\right]}{\left[\frac{\lambda_n^2}{(R-1)^2}+N^2\right]\left[\sin\lambda_n\right]\left\{\frac{4\left[P_i^2+1\right]^2\lambda_n}{2B_i\left[P_i^2+1\right]+1}+\frac{2\left[P_i^2+1\right](R-1)+2B_i\left(P_i^2+1\right)(R-1)^2+(R-1)^2}{\lambda_n}\right\}} \tag{15}$$

From an examination of Eq. 15, it cab be easily seen that the value of the temperature reaches within one percent of its steady state value when the end of fin (ξ = R) with the following condition holds,

$$\frac{2e^{-\left[\frac{\lambda_1^2}{(R-1)^2}+N^2\right]\tau}\left\{2N\left[P_i^2+1\right]\sinh\left[N(R-1)\right]+2\left[B_i\left(P_i^2+1\right)+1\right]\cdot\cosh\left[N(R-1)\right]\right\}}{\left[\frac{\lambda_1^2}{(R-1)^2}+N^2\right]\left[\sin\lambda_1\right]\left\{\frac{4\left[P_i^2+1\right]^2\lambda_1}{2B_i\left[P_i^2+1\right]+1}+\frac{2\left[P_i^2+1\right](R-1)+(R-1)^2}{\lambda_1}+\frac{2B_i\left[P_i^2+1\right](R-1)^2}{\lambda_1}\right\}}<0.01 \tag{16}$$

or express as another form,

$$\tau>\frac{1}{\left[\frac{\lambda_1^2}{(R-1)^2}+N^2\right]}\ell n\left\{\frac{\left\{200\left\{2N\left[P_i^2+1\right]\sinh\left[N(R-1)\right]+\left[2B_i\left(P_i^2+1\right)+1\right]\cosh\left[N(R-1)\right]\right\}\right\}}{\left\{\left[\frac{\lambda_1^2}{(R-1)^2}+N^2\right]\left\{\frac{4\left[P_i^2+1\right]^2\lambda_1}{2B_i\left[P_i^2+1\right]+1}+\frac{(R-1)^2}{\lambda_1}+\frac{2\left[P_i^2+1\right](R-1)+2B_i\left[P_i^2+1\right](R-1)^2}{\lambda_1}\right\}\left[\sin\lambda_1\right]\right\}}\right\} \tag{17}$$

where, λ_1 is the first root of Eq. 14. The minimum value of time that is needed to reach the steady state τ_{min} can be obtained from Eq. 17. Defining the non-dimensional heat flux at the fin base as:

$$q_0^* = q_b r_1 / 4k \ [\delta \pi r_1] \ [T_f - T_\infty] \tag{18}$$

After employing the non-dimensional parameters, the heat flux can be expresses as:

$$q_0^* = -\sqrt{P_i^2 + 1}\frac{\partial \phi}{\partial \xi}(1, \tau), \ \tau > 0 \tag{19}$$

After applying the temperature distribution $\phi(\xi, \tau)$ in Eq. 15, the non-dimensional heat flux at the base of spiral fin is given by:

$$q_0^* = \frac{2B_i\sqrt{P_i^2+1}\left\{N\sinh\left[N(R-1)\left[P_i^2+1\right]+1/2\cosh\left[N(R-1)\right]\right]\right\}}{2N\left[P_i^2+1\right]\sinh\left[N(R-1)\right]+\left[2B_i\left(P_i^2+1\right)+1\right]\cosh\left[N(R-1)\right]}$$
$$+\frac{8B_i^2\left[P_i^2+1\right]^{5/2}}{(R-1)\left[2B_i\left(P_i^2+1\right)+1\right]}\sum_{n=1}^{\infty}\frac{\lambda_n \cdot e^{-\left[\frac{\lambda_n^2}{(R-1)^2}\right]\tau}}{\left\{\left[\frac{\lambda_n^2}{(R-1)^2}+N^2\right]\left\{\frac{4\left[P_i^2+1\right]^2\lambda_n}{2B_i\left[P_i^2+1\right]+1}+\frac{2\left[P_i^2+1\right](R-1)+(R-1)^2}{\lambda_n}+\frac{2B_i\left[P_i^2+1\right](R-1)^2}{\lambda_n}\right\}\right\}} \tag{20}$$

Case 2: A sinusoidal with unit amplitude in base fluid temperature: The temperature variation of the fluid has been changed as $T_f = T_0 + T_A \sin \tilde{\omega} t$ and the non-dimensional parameters for the temperature distribution and frequency are

$$\Gamma = \frac{T - T_\infty}{T_A}, \quad \Gamma_0 = \frac{T_0 - T_\infty}{T_A}, \quad \omega = \frac{\tilde{\omega} r_1^2}{\alpha}$$

With the temperature distribution of the spiral fin now was replaced by the symbol of Γ. Therefore, the governing equation is:

$$\frac{\partial}{\partial \xi}\left\{\sqrt{P_i^2+\xi^2}\frac{\partial \Gamma}{\partial \xi}\right\} - N^2\sqrt{P_i^2+\xi^2}\Gamma = \sqrt{P_i^2+\xi^2}\frac{\partial \Gamma}{\partial \tau}, \ \tau > 0, \ 1 < \xi < R \tag{21}$$

The boundary condition (4) is expressed as:

$$-\frac{\partial \Gamma}{\partial \xi} + B_i\Gamma = B_i\left(\sin \omega\tau + \Gamma_0\right), \ \xi = 1, \ \tau > 0 \tag{22}$$

The boundary condition (5) and the initial condition (3) can be expressed as:

$$\frac{\partial \Gamma}{\partial \xi}(R, \tau) = 0, \ \tau > 0, \qquad \Gamma(\xi, 0) = 0, \ 1 < \xi < R \tag{23}$$

Following the same procedure as in the Case 1 by taking the Laplace Transformation with respect to τ for Eq. 21 and 22, and using the Keller and Keller's method, the governing differential equation is:

$$\overline{\Gamma}(\xi, s) = F_2\left\{-\left[N^2+s\right]\left[P_i^2+\xi^2\right]\right\}^{-1/4}\cosh\left[\sqrt{N^2+s}\cdot(R-\xi)\right] \tag{24}$$

where, F_2 is a constant. After employing the Laplace transform, the boundary condition (22) can be expressed as:

$$\frac{\partial \overline{\Gamma}}{\partial \xi} + B_i\overline{\Gamma} = \frac{B_i\omega}{s^2+\omega^2}, \qquad \xi = 1 \tag{25}$$

Taking the differentiation of Eq. 24 with respect to ξ and substituting the result into Eq. 25, the constant F_2 can be obtained as:

$$F_2 = \frac{2B_i\omega\left[-\left(N^2+1\right)\right]^{1/4}}{s^2+\omega^2}\cdot\frac{\cosh\left[\sqrt{N^2+s}\left(R-\xi\right)\right]}{\left\{2\left[P_i^2+1\right]\sqrt{N^2+s}\sinh\left[\sqrt{N^2+s}\left(R+1\right)\right]+\left[P_i^2+1\right]\cdot\cosh\left[\sqrt{N^2+s}\left(R-1\right)\right]\cdot\left[2B_i\left(P_i^2+1\right)+1\right]\right.} \tag{26}$$

Therefore, the temperature distribution in s domain is:

$$\overline{\Gamma}\left(\xi,s\right) = \frac{2B_i\omega\left[P_i^2+1\right]^{5/4}}{\left(P_i^2+\xi^2\right)^{1/4}\cdot\left(s^2+\omega^2\right)}\cdot\frac{\cosh\left[\sqrt{N^2+s}\left(R-\xi\right)\right]}{\left\{2\left[P_i^2+1\right]\cdot\sqrt{N^2+s}\cdot\sinh\left[\sqrt{N^2+s}\cdot\left(R-1\right)\right]+\left[2B_i\left(P_i^2+1\right)+1\right]\cdot\cosh\left[\sqrt{N^2+s}\cdot\left(R-1\right)\right]\right\}} \tag{27}$$

The inverse transform is obtained by using the contour integral method and taking the inverse of Laplace transform, the result is:

$$\Gamma\left(\xi,\tau\right) = \frac{1}{2\pi i}\int_{r-i\infty}^{r+i\infty}\frac{2B_i\left[P_i^2+1\right]^{5/4}\cdot\omega\cdot e^{\tau^2}}{\left[P_i^2+\xi^2\right]^{1/4}\left[z^2+\omega^2\right]}\cdot\left\{\frac{\cosh\left[\sqrt{N^2+z}\cdot\left(R-\xi\right)\right]}{2\left(P_i^2+1\right)\sqrt{N^2+z}\cdot\sinh\left[\sqrt{N^2+z}\left(R-1\right)\right]+\left[2Bi\left(P_i^2+1\right)+1\right]}\right\}dz\cdot\cosh\left[\sqrt{N^2+z}\left(R-1\right)\right] \tag{28}$$

where the first tem, second term and third term can be respectively expressed as:

$$R_{es}\left(i\omega\right) = \frac{B_i\left[P_i^2+1\right]^{5/4}e^{i\omega\tau}}{i\left[P_i^2+\xi^2\right]^{1/4}}\cdot\left\{\frac{\cosh\sqrt{N^2+i\omega}\left(R-\xi\right)}{2\left[P_i^2+1\right]\sqrt{N^2+i\omega}\sinh\left[\sqrt{N^2+i\omega}\left(R-1\right)\right]+\left[2B_i\left(P_i^2+1\right)+1\right]}\right\}\cdot\cosh\left[\sqrt{N^2+i\omega}\left(R-1\right)\right] \tag{29}$$

And

$$R_{es}\left(-i\omega\right) = -\frac{B_i\left[P_i^2+1\right]^{5/4}e^{i\omega\tau}}{i\left[P_i^2+\xi^2\right]^{1/4}}\cdot\left\{\frac{\cosh\sqrt{N^2-i\omega}\left(R-\xi\right)}{2\left[P_i^2+1\right]\sqrt{N^2-i\omega}\sinh\left[\sqrt{N^2-i\omega}\left(R-1\right)\right]+\left[2B_i\left(P_i^2+1\right)+1\right]\cdot\cosh\left[\sqrt{N^2-i\omega}\left(R-1\right)\right]}\right\} \tag{30}$$

And

$$\sum_{n=1}^{\infty}R_{es}\left(z_{on}\right) = \frac{4B_i\left[P_i^2+1\right]^{5/4}\omega}{\left[P_i^2+\xi^2\right]^{1/4}}\cdot\sum_{n=1}^{\infty}\frac{e^{-\left[\frac{\lambda_n^2}{(R-1)^2}+N^2\right]\tau}\cdot\cos\left[\lambda_n\left(\frac{R-\xi}{R-1}\right)\right]}{\left\{\omega^2+\left[\frac{\lambda_n^2}{\left(R-1\right)^2}+N^2\right]^2\right\}\left\{\frac{4\left[P_i^2+1\right]^2\lambda_n}{2B_i\left(P_i^2+1\right)+1}+\frac{2\left[P_i^2+1\right]\left(R-1\right)}{\lambda_n}+\frac{2B_i\left(P_i^2+1\right)\left(R-1\right)^2+\left(R-1\right)^2}{\lambda_n}\right\}\left[\sin\lambda_n\right]} \tag{31}$$

And λ_n's in Eq. 30 are the same as the solutions of Eq. 14. Introducing the defined parameters

$$g = \sqrt{N^4+\omega^2\left(R-1\right)^2};\qquad \beta = \frac{1}{2}\tan^{-1}\left(\omega/N^2\right)$$

$$a = \sqrt{g}\cos\beta;\qquad b = \sqrt{g}\sin\beta$$

The first and second terms in the temperature distribution can be combined and expressed as :

$$R_{es}\left(i\omega\right)+R_{es}\left(-i\omega\right) = \frac{2B_i\left[P_i^2+1\right]^{5/4}\left[BC-AD\right]}{\left[P_i^2+\xi^2\right]^{1/4}\left[C^2+D^2\right]} = A'_{mt}\sin\left(\omega\tau-\phi'_t\right) \tag{32}$$

where the A, B, C, D, are defined as the followings:

$A = \cos\omega\tau \cdot \cosh aX \cdot \cos bX - \sin\omega\tau \cdot \sinh aX \cdot \sin bX$
$B = \cos\omega\tau \cdot \cosh aX \cdot \cos bX + \sin\omega\tau \cdot \cosh aX \cdot \cos bX$
$C = V \cdot a \cdot \sinh a \cdot \cos b - V \cdot b \cdot \cosh a \cdot \sin b + W \cdot \cosh a \cdot \cos b$
$C = V \cdot a \cdot \sinh a \cdot \cos b + V \cdot b \cdot \cosh a \cdot \sin b + W \cdot \cosh a \cdot \cos b$

and

$$X = \frac{R-\xi}{R-1}, \qquad V = \frac{2\left(P_i^2+1\right)}{(R-1)}, \qquad \omega = 2B_i\left(P_i^2+1\right)+1$$

Therefore, the phase angle of the temperature distribution ϕ_t' is:

$$\phi_t' = \tan^{-1}\left\{\frac{\cosh aX \cdot \cos bX \cdot D - \sinh aX \cdot \sin bX \cdot C}{\cosh aX \cdot \cos bX \cdot C + \sinh aX \cdot \sin bX \cdot D}\right\} \tag{33}$$

The amplitude of the temperature distribution A'_{mt} is:

$$A'_{mt} = \frac{2B_i\left[P_i^2+1\right]^{5/4}}{\left[P_i^2+\xi^2\right]^{1/4}} \frac{1}{\left[C^2+D^2\right]} \sqrt{N_r^2+D_r^2} \tag{34}$$

where, N_r and D_r represent the numerator and denominator in Eq. 32, respectively. The temperature response is then given by the sum of Eq. 31 and 32. Equation 31 represents the material transient response temperature distribution immediately after the base is subjected to the oscillating base fluid temperature with unit amplitude. And Eq. 32 represents the steady periodic response temperature distribution to the oscillating base fluid temperature with unit amplitude. Introducing the same definition for the heat flux as in the Case 1, the heat flux is defined as:

$$q^{*}_{a} = q_b \cdot r_1/4k \left[\delta\, \pi\, \Gamma_1\right] T_A \tag{35}$$

After the Laplace transform, the heat flux is:

$$q^{*}_{a} = -\sqrt{P_i^2+1}\frac{\partial\Gamma}{\partial\xi}(1,\tau) \tag{36}$$

Applying the temperature distribution from the sum of Eq. 31 and 32, the non-dimensional heat flux at the fin base with a sinusoidal fluid temperature of unit amplitude can be obtained as:

$$q_a^*(1,\pi) = A'_{mq}\sin\left(\omega\tau - \phi'_q\right) - \frac{8\omega B_i^2\left[P_i^2+1\right]^{5/2}}{\left[2B_i\left(P_i^2+1\right)+1\right](R-1)} \cdot \sum_{n=1}^{\infty} \frac{\lambda_n \cdot e^{-\left[\frac{\lambda_n^2}{(R-1)^2}+N^2\right]\tau}}{\left\{\omega^2+\left[\frac{\lambda_n^2}{(R-1)^2}+N^2\right]^2\right\}\left\{\frac{4\left[P_i^2+1\right]^2\lambda_n}{2B_i\left[P_i^2+1\right]+1} + \frac{2\left[P_i^2+1\right](R-1)}{\lambda_n} + \frac{2B_i\left[P_i^2+1\right](R-1)^2+(R-1)^2}{\lambda_n}\right\}} \tag{37}$$

where the phase angle under steady state condition ϕ_q' can be shown as:

$$\phi'_q = \tan^{-1}\left\{\frac{Q - 2Z_2\left[P_i^2+1\right]/[R-1]}{P - 2Z_1\left[P_i^2+1\right]/[R-1]}\right\} \tag{38}$$

where the symbols P, Q, Z_1 and Z_2 denote, respectively, as:

$P = \cosha \cdot \cosb \cdot C + \sinha \cdot \sinb \cdot D$

$Q = \cosha \cdot \cosb \cdot C - \sinha \cdot \sinb \cdot C$

$Z_1 = a \cdot C \cdot \sinha \cdot \cosb - b \cdot C \cdot \cosha \cdot \sinb + a \cdot D \cdot \cosha \cdot \sinb + b \cdot D \cdot \sinha \cdot \cosb$

$Z_2 = a \cdot C \cdot \sinha \cdot \cosb + b \cdot C \cdot \cosha \cdot \sinb - a \cdot D \cdot \cosha \cdot \sinb + b \cdot D \cdot \sinha \cdot \cosb$

The symbols C and D are defined as before. Meanwhile, the amplitude under steady state conditions A'_{mq} is:

$$A'_{mq} = \left\{B_i\sqrt{P_i^2+1} \Big/ \left[C^2+D^2\right]\right\}\sqrt{N_{rq}^2+D_{rq}^2} \quad (39)$$

where, N_{rq} and D_{rq} represent the numerator and denominator in Eq. 38, respectively. In Eq. 37, the first term represents the steady periodic response base heat flux to the oscillating base fluid temperature with unit amplitude. And the second terms represent the initial transient response base heat flow.

RESULTS AND DISCUSSION

Case 1: A unit step change in base fluid temperature: The temperature distribution of the spiral fin ϕ obtained from Eq. 15 is plotted in Fig. 2-5 for different values of τ, B_i, N, P_i and R.

The result can be draw from Fig. 2-5 that the temperature distribution ϕ increase as the time elapsed. Also, the absolute slope of temperature distribution ϕ of the spiral fin base has a trend of decreasing with an increase of time τ which implies that the output heat flux in base of fin will be decreased with an increase of time τ. This result is due to the increase of internal temperature of the spiral fin when time τ is increasing. Meanwhile, for the greater values of fin pitch P_i, the greater values of temperature distribution ϕ will be at the same values of B_i, R, τ and N except for very small values of time τ and very large values of N.

It can be seen that the greater the value of B_i, the greater the temperature distribution ϕ will be at the same values of P_i, N, τ and R by comparing Fig. 2 and 3. The temperature distribution ϕ is a function of B_i because of the heat flux at fin base transferred from convection is larger for the large values of B_i.

It can be seen that the larger the values of N, the smaller the temperature distribution ϕ at the same values of P_i, τ, R and B_i in comparing the Fig. 3 and 4. Also, from Fig. 3 and 5, it can be seen that the same trend as R increases, the temperature distribution ϕ decreases at the same value of B_i τ, P_i and N.

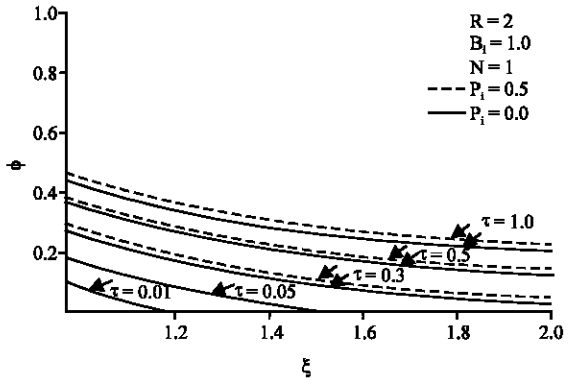

Fig. 2: The temperature distribution for R-2, N = 1 B_i =1.0

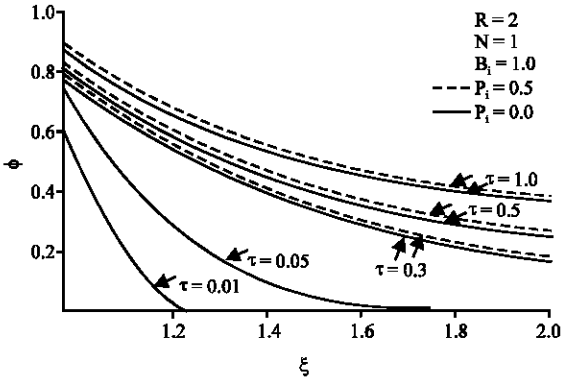

Fig. 3: The temperature distribution for R = 2, N = 1 B_i = 10

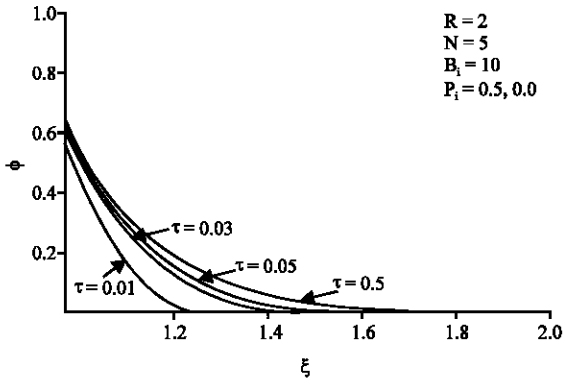

Fig. 4: The temperature distribution for R = 2, N = 5 B_i = 10

The dimensionless time for reaching the steady state τ_{min} with different parameters of τ, B_i, N, P_i and R of Eq. 17, is plotted in Fig. 6 and 7 and discussed as in the followings. From these two plots, the τ_{min} decreases at the same N due to the increase of heat flux at the fin base for the increase of B_i. When the B_i becomes very large, the boundary condition of the fin base can be treated as $-\partial\phi/\partial\xi + B_i\,\phi = B_i$ of which is approximated as $\Phi \simeq 1$. This is just the same as the fin base under the condition

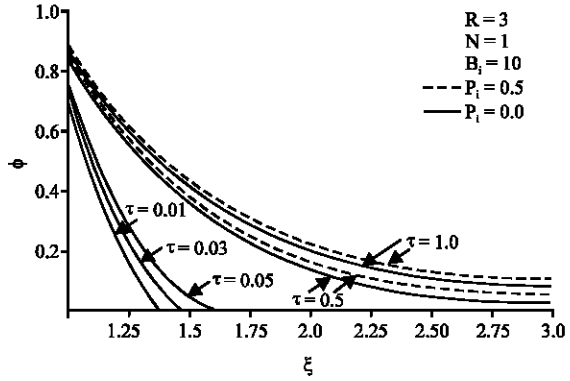

Fig. 5: The temperature distribution for R = 3, N = 1 B_i = 10

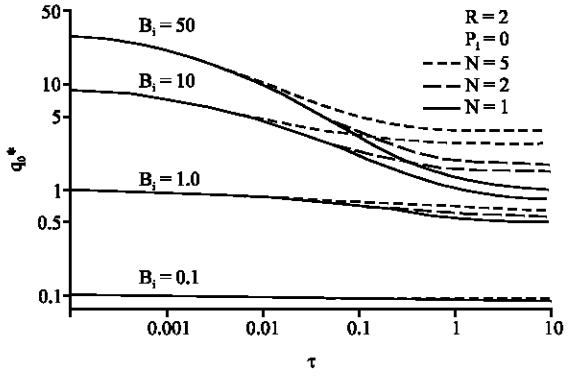

Fig. 8: The heat flux distribution for R = 2, P_i = 0

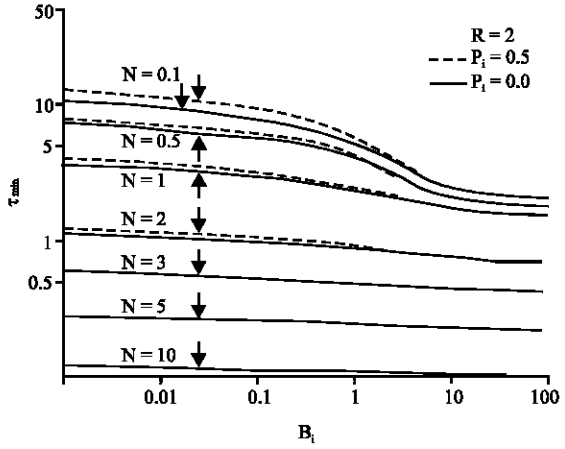

Fig. 6: The temperature distribution for R = 2 and unit step input

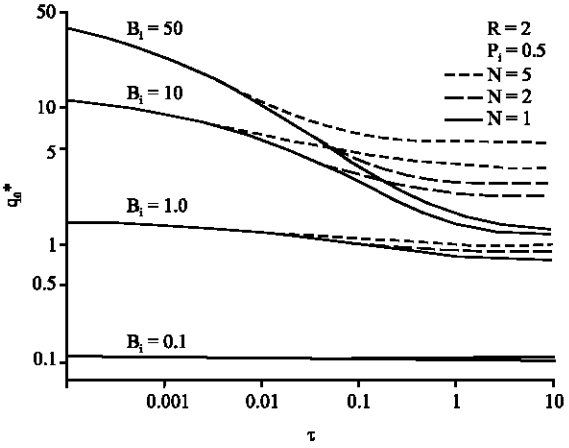

Fig. 9: The heat flux distribution for R=2, Pi=0.5

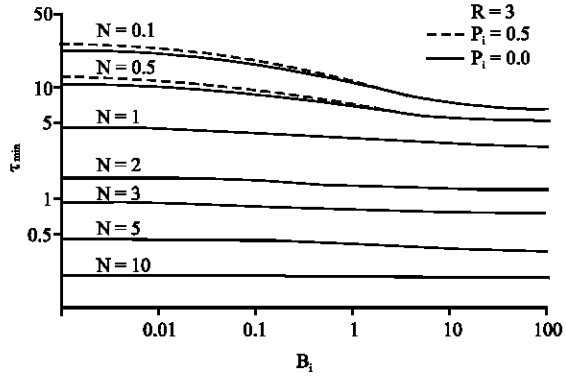

Fig. 7: The time constant distribution for R = 3 and unit step input

of a unit step change in base temperature. This result can be obtained from fact that τ_{min} is almost the same at R = 2 and R = 3 for the case of B_i is greater than 50. Also, the dimensionless time is needed to reach the steady state τ_{min} for different N showed that τ_{min} decreased as the N increased when the other parameters hold the same. However, the opposite trend is found in the parameter R, as the τ_{min} increased when the R increased. And the τ_{min} increased as P_i increased except for the cases of very large N or B_i. The difference of τ_{min} with different values of P_i decreased with the increase of B_i and gradually reached to zero. It implied that the τ_{min} is not a function of P_i when ϕ = 1.

The heat flux at the fin base q_0^* with different parameters of τ, B_i, N, P_i and R of Eq. 20 is plotted in Fig. 8-11. The heat flux at fin base is not affected by the τ when examining the Fig. 8, 9 and 11 for the very small values of dimensionless time τ. It is because that different values of N represented the different values of convective heat transfer coefficient for the same shape and size of the spiral fin. Initially the heat flux transferred into the fin by the fin base was used to increase the internal energy of the spiral fin itself. Therefore, the heat flux q_0^* had little effect on the fin. This is same situation happened in the case of a unit step change of the temperature in fin base.

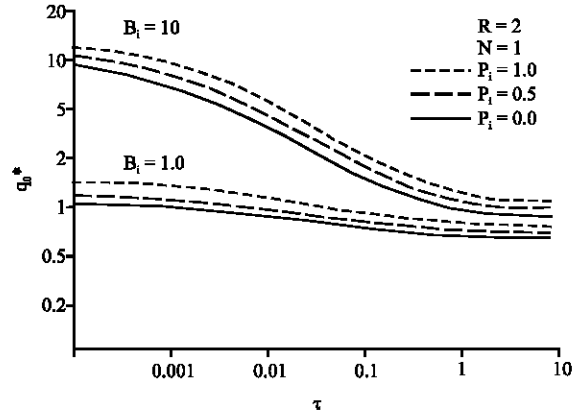

Fig. 10: The heat flux distribution for R = 2, N = 1, with different P_i

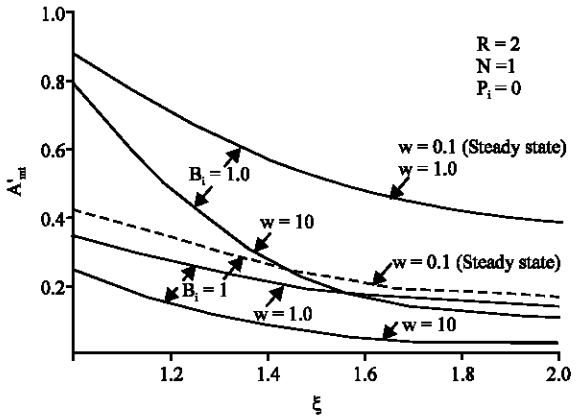

Fig. 12: The temperature distribution for amplitude at R = 2, N = 1, P_i = 0

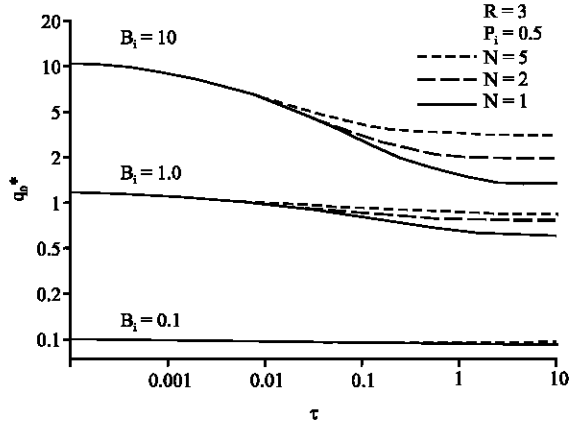

Fig. 11: The heat flux distribution for R = 3, P_i = 0.5 with different N

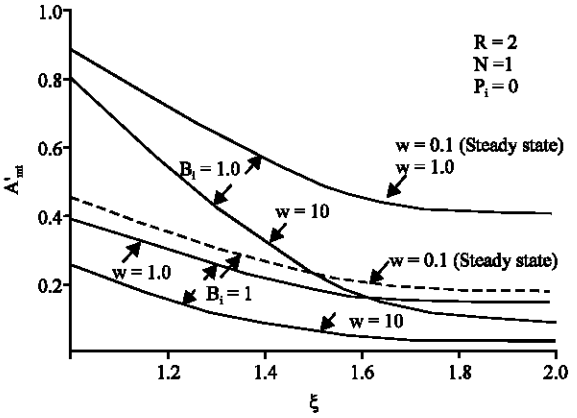

Fig. 13: The temperature distribution for amplitude at R = 2, N = 1, P_i = 0.5

Comparing the Fig. 8-11, the heat flux at the beginning can be represented by the equation $-\partial\phi/\partial\xi = B_i$ because the low temperature at fin base when the boundary condition is $-\partial\phi/\partial\xi + B_i\,\phi = B_i$. Therefore, both the temperature distribution ϕ and the heat flux of fin base q_0* increased as the B_i increased for the same values of R, τ, N, P_i from the plots of Fig. 2 and 3. When the values of B_i is larger than 50, the situation can be simulated as the case of a unit step change in fin base temperature. But the heat flux at fin base q_0* for the variation of fluid temperature is smaller than the heat flux obtained from the case of a unit step change in the fine base temperature. Due to the fluid convective resistance, q_0* is smaller than the special case. Although, it showed that at the beginning, the heat flux at fin base is not affected by R. However, the heat flux at fin base q_0* would increase as the values of N or R increased by keeping the other parameters unchanged. Also, it showed the parameter P_i has the same trend as the parameters of N and R.

Case 2: A sinusoidal with unit amplitude in base fluid temperature: The temperature response is then given by the sum of Eq. 31 and 32. Equation 31 represents the material transient response temperature immediately after the base is subjected to the oscillating base fluid temperature with unit amplitude. And Eq. 32 represents the steady periodic response temperature to the oscillating base fluid temperature with unit amplitude.

Only the steady term of the temperature distribution is on interested in the present study. The phase angle ϕ_t' and amplitude A_{mt}' of temperature distribution of the spiral fin Γ obtained from Eq. 33 and 34 are plotted in Fig. 12-18 for different values of ω, B_i, N, P_i and R.

Figure 12-18 showed that the amplitude A_{mt}' of fin base temperature distribution Γ at low frequency can be

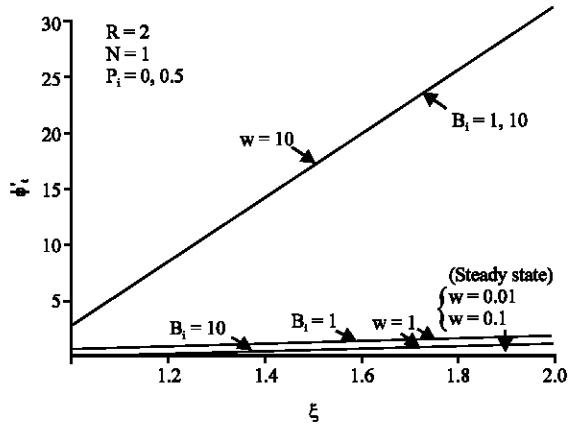

Fig. 14: The phase angle distribution at R = 2, N = 1, P_i = 0 and 0.5

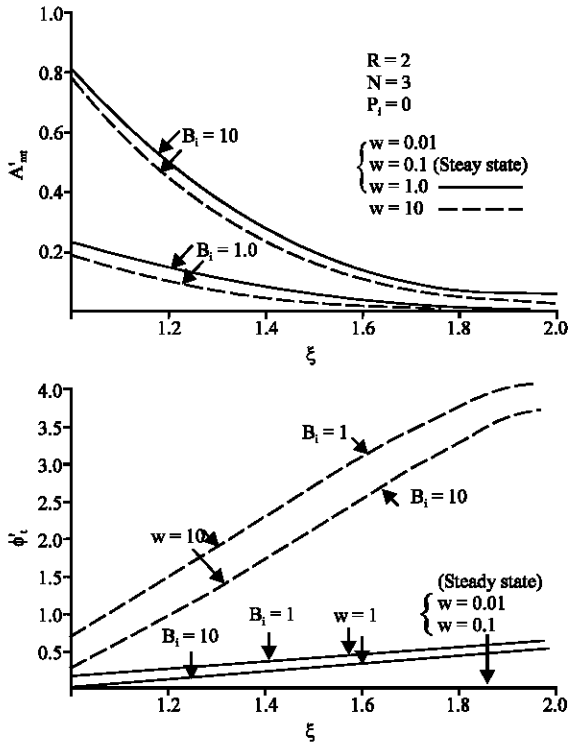

Fig. 15: The amplitude and phase angle of temperature distribution at R = 2, N = 3, P_i = 0

approximated as the case 1 of whish the fin base is subjected to a variation of unit step change in fluid temperature. Also, it showed that the amplitude A_{mt}' of temperature distribution Γ increased as the B_i increased for the same values of P_i, N, ω and R. But the amplitude A_{mt}' of temperature distribution Γ decreased as the N increased. Also the amplitude A_{mt}' of temperature distribution Γ increased as the P_i increased except for the

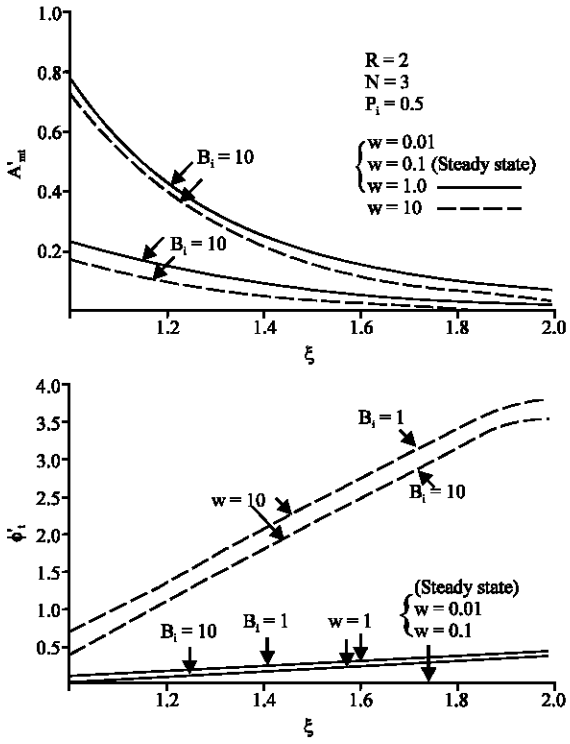

Fig. 16: The amplitude and phase angle of temperature distribution at R = 2, N = 3, P_i = 0.5

very large values of N. Because of its larger importance of the convective heat transfer between the spiral fin and the fluid than the shape of fin itself, the influence of N is greater than P_i on the amplitude A'_{mt} of temperature distribution.

The effect of the frequency can be obtained from Fig. 12-18. The amplitude A_{mt}' of temperature distribution Γ decreased as the values of ω increased for the same values of B_i, N, P_i and R. Because the Eq. 34 can be expanded in the form of a Fourier series and the largest ω can be decided from the boundary condition. Therefore, the higher order terms can be transacted for the frequency larger than the largest value of ω. And the error can be estimated from the finite terms.

Figure 12-18 also showed that the phase angle ϕ_t' of fin base temperature distribution Γ for the different values of P_i, Bi, N, ω and R. The phase angle ϕ_t' of temperature distribution Γ decreased as the N increased for the same values of P_i, B_i, ω and R.

The heat flux at the fin base q_a^* with different parameters of ω, B_i, N, P_i and R of is shown in Eq. 37. Only the steady term of the temperature distribution is on interested, however. The phase angle ϕ_t' and amplitude A_{mt}' of temperature distribution of the spiral fin q_a^* obtained from Eq. 38 and 39 are plotted in Fig. 19-22 for

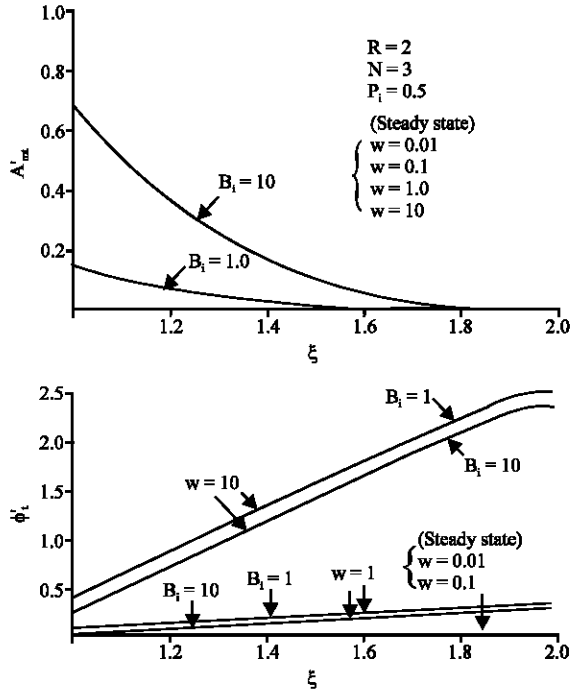

Fig. 17: The amplitude and phase angle of temperature distribution at R = 2, N = 5, P_i = 0

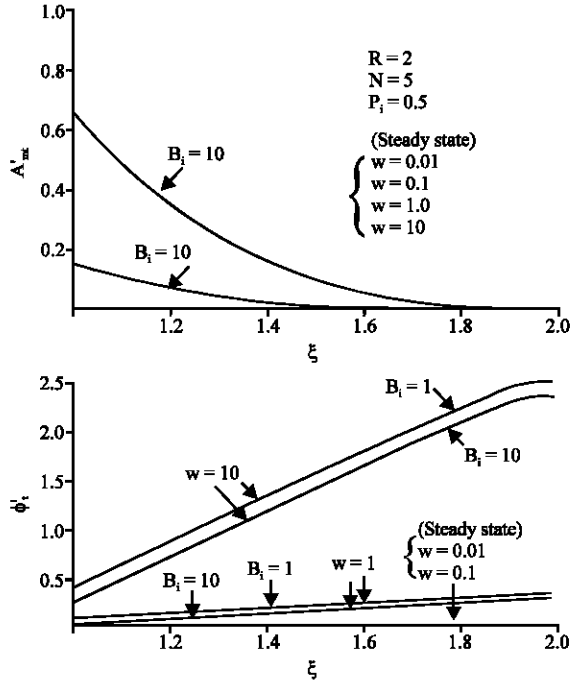

Fig. 18: The amplitude and phase angle of temperature distribution at R = 2, N = 5, P_i = 0.5

different values of ω, B_i, N, P_i and R. Figure 19 and 20 showed that the amplitude A_{mt}' of the heat flux q_a^*

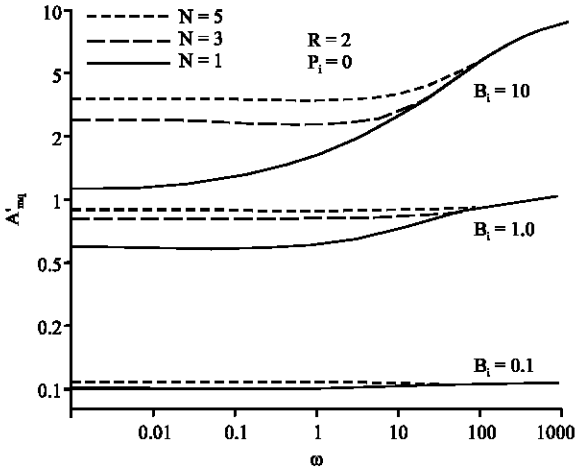

Fig. 19: The amplitude and phase angle of temperature distribution at R = 2, P_i = 0

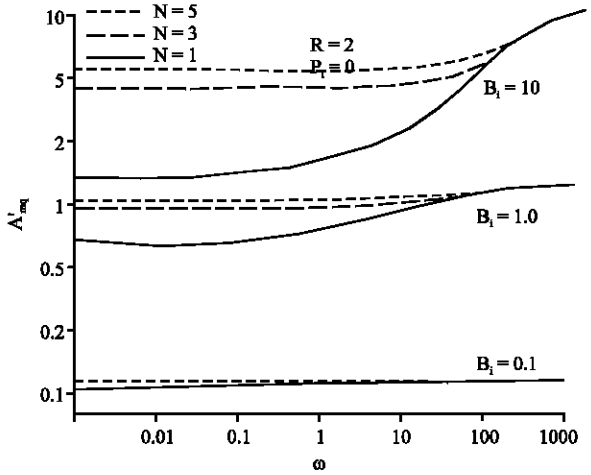

Fig. 20: The amplitude and phase angle of temperature distribution at R = 2, P_i = 0.5

increased as the input oscillating frequency ω increased except for the very small values of B_i at different values of N, P_i and R. Also, the amplitude A_{mt}' of the heat flux q_a^* increased as the values of B_i increased. And the amplitude A_{mt}' of the heat flux q_a^* increased as the values of N increased except for the small values of ω, for example ω is smaller than 50, too.

Figure 21 showed that the amplitude A_{mt}' of the heat flux q_a^* increased as the values of P_i increased for different values of N, B_i, ω and R. Also, Fig. 22 showed that the amplitude A_{mt}' of the heat flux q_a^* increased as the values of R increased for different values of N, B_i, ω and P_i except for the very large values of ω.

From above, we can obtain the features that the amplitude A_{mt}' of the heat flux q_a^* at any point in the spiral

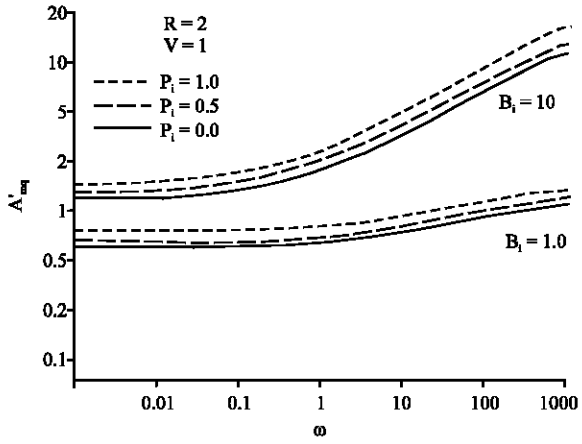

Fig. 21: The amplitude and phase angle of temperature distribution at R = 2, N = 1 with different P_i

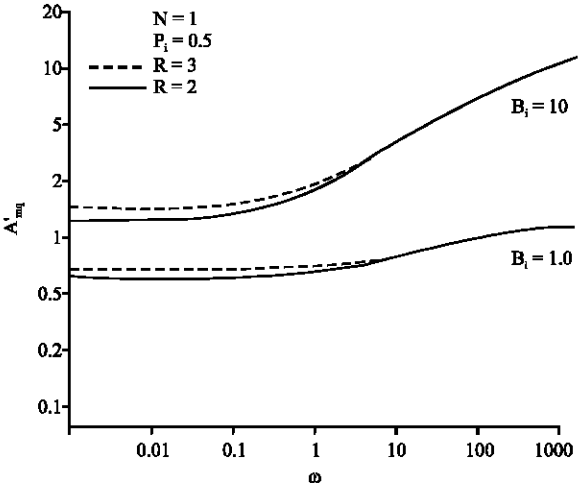

Fig. 22: The amplitude and phase angle of temperature distribution at, N = 1, P_i = 0.5

fin of this case is approximately the same as those in the case to a step change in the base temperature for the steady state situation and the low oscillating frequency of which is $\omega \leq 1$. However, the greater the values of P_i, the greater the values of the amplitude A_{mt}' of the heat flux q_a* temperature response at the same values of ω, R, B_i and N. Although the deviation the amplitude A_{mt}' with different values of P_i is less sensitive than those of N, but it also contributes its part in enhancing the heat transfer effect.

CONCLUSIONS

From the case 1, a variation with a unit step change in base heat flux, it can be seen that the large the values of N, the smaller the values of temperature response at the same values of τ, P_i and R. In addition, the greater the values of P_i, the higher the values of temperature response at the same values of N, R and τ. Also it can conclude that the greater the values of R, the smaller the values of temperature response at the same values of τ, N and P_i. It can be seen that τ_{min} decreases with an increase of N at the same values of P_i and R. It also can be seen that the time for reaching steady state, τ_{min}, increases with an increase of R at the same values of N and P_i and P_i at the same values of N and R.

From the case 2, a variation with a sinusoidal base heat flux with unit amplitude e know that the greater the values of N, the smaller the values of temperature response amplitude at the same values of P_i, ω and R; in addition, the higher values of oscillating frequency, the smaller the values of temperature response amplitude at the same values of P_i, R and N. It also can be seen that the greater the values of P_i, the greater the values of temperature response amplitude at the same values of N, ω and R. Also it can conclude that the greater the values of R, the smaller the temperature response amplitude at the same values of N, P_i and ω in a similarity shape of radial dimension in R. However, the temperature response phase angle decreases with an increase of N at the same values of P_i, ω and R. The temperature response angle also increases with an increase of ω for keeping the other conditions in the same values.

In this study, the exact transient solution for unit step input and sinusoidal base heat flux has been obtained. From the results of the above cases, it can be found that the temperature response at the fin base will be influenced by the frequency. Also the amplitude of the input temperature has the direct impact on the time constant for both cases. However, the dominant parameters of P_i, R and N would be the major factors in represented the response of the heat transfer from the base to the spiral fin. These results can be used as the foundation in applying the spiral fin on the industry.

ACKNOWLEDGMENT

The current authors gratefully acknowledge the financial support provided to this study by the National Science Council of Taiwan under Grant No. NSC 95-2221-E-167-028 and NSC 95-2622-E-167-010-CC3.

NOMENCLATURE

A'_{mq} = Dimensionless base heat flow amplitude under steady state

A'_{mt} = Dimensionless temperature amplitude

$B_i = h_f r_1/k_f$ = Biot number
c = Specific heat for material of fin
h = Convective heat transfer coefficient surronding fin
h_f = Base convective heat transfer coefficient
k = Thermal conductivity for material of fin
k_f = Thermal conductivity of fluid for fin base
N = $[hr_1^2/k\delta]^{1/2}$
p = Pitch of spiral fin
p_i = Dimensionless of pitch $[p/2\pi r_1]$
q_b = Heat flow at base of fin
q_b^* = Dimensionless base heat flow $[q_b r_1/k(4\delta\pi r_1)(T_f-T_\infty)]$
q_a^* = Dimensionless base heat flow Eq. 31
r = Radius of concerned fin
r_1 = Inner radius of fin
r_2 = Outer radius of fin
$R = r_2/r_1$ = Dimensionless radius
t = Time
T = Temperature of fin
T_A = Temperature parameter
T_f = Base fluid temperature
T_0 = Temperature parameter
T_∞ = Temperature of fluid surrounding fin
X = Dimensionless radial parameter $[(R-\xi)/(1-1)]$
α = Thermal diffusivity $[k/\rho c]$
δ = Half thickness of uniform fin
ρ = Density for material of fin
ϕ = Dimensionless temperature $[(T-T\infty)/T_f-T_\infty)]$
Γ = Dimensionless temperature $[(T-T_\infty)/T_A)]$
Γ_0 = Dimensionless temperature parameter $[(T-T_\infty)/T_A)]$
τ = Dimensionless time
ξ = Dimensionless radius
ω = Dimensionless frequency of oscillation $[\varpi r_1^2/\alpha]$
ϖ = Frequency of oscillation
ϕ_q' = Base heat flow phase angle under steady state
ϕ_t' = Temperature phase angle

REFERENCES

Campo, A. and R.E. Stuffle, 1996. Symbolic mathematics for calculation of thermal efficiencies and tip temperatures in annual fins of uniform thickness. Int. J. Heat Mass Transfer, 40 (2): 490-492.

Chu, Hsin-Sen, Chao-Kuang Chen and Cheng-I Weng, 1982. Applications of fourier series technique to transient heat transfer problem. J. Chem. Eng. Commun., 16 (1): 215-225.

Chu, Hsin-Sen, Chao-Kuang Chen and Cheng-I Weng, 1983a. Transient response of circular pins. ASME. J. Heat Transfer, 105 (1): 205-208.

Chu, Hsin-Sen, Cheng-I Weng and Chao-Kuang Chen, 1983b. Transient response of a composite straight fin. ASME. J. Heat Transfer, 105 (2): 307-311.

Cheng, Ching-Yang and Chao-Kuang Chen, 1994. Transient response of annular fins of various shapes subjected to constant base heat fluxes. J. Phys. D: Applied Phys., 27 (11): 2302-2306.

Cheng, Ching-Yang and Chao-Kuang Chen, 1998. Transient response of annular fins subjected to constant base temperatures. Int. Commun. Heat Mass Transfer, 25 (6): 775-785.

Crank, J. and I.B. Parker, 1966. Approximate methods for two dimensional problems in heat flow. Q. J. Mech. Applied Math., 19 (2): 167-181.

Harper, D.R. and W.B. Brown, 1992. Mathematical Equations for Heat Conduction in the Fins of Air Cooled Engines. NACA Report, 158.

Keller, H.B. and J.B. Keller, 1962. Exponential-like solutions of system of ordinary differential equations. J. Soc. Ind. Applied Math., 10 (1): 246-259.

Laor, K. and H. Kalman, 1996. Performance and optimum dimensions of different cooling fins with a temperature dependent heat transfer coefficient. Int. J. Heat Mass Transfer, 39 (9): 1993-2003.

Luo, W.J. and R.J. Yang, 2007. Flow bifurcations and heat transfer in a two sides lids-driven cavity. Int. J. Heat Mass Transfer, 50 (11): 2394-2405.

Mokheimer, E.M.A., 2002. Performance of annual fins with different profiles subject to variable heat transfer coefficient. Int. J. Heat Mass Transfer, 45 (17): 3631-3642.

Ozisik, M.N., 1980. Heat Conduction. John Wiley and Sons, Inc., New York.

Park, K., K.H. Rew, J.T. Kwon and B.S. Kim, 2007. Optimal solutions of pin-fin type heat sinks for different fin shapes. J. Enhanced Heat Transfer, 14 (2) 93-104.

Shih, M.H., W.J. Luo and K.C. Yu, 2008. Evaporation of non-newtonian fluid porous medium under mixed convection. J. Mech., 24 (2): 79-87.

T'joen, C., A. Willockx, H.J. Steeman and M. De Paepe, 2007. Performance prediction of compact fin-and-tube heat exchangers in maldistributed airflow. Heat Transfer Eng., 28 (12): 986-996.

Yu, Lien-Tsai and Cha'o-Kuang Chen, 1999. Application of the taylor transformation to the transient temperature response of an annular fin. Heat Transfer Eng., 20 (1): 78-87.

Zubair, S.M., A.Z. Al-gami and J.S. Nizami, 1996. The optimal dimensions of circular fins with variable profile and temperature-dependent thermal conductivity. Int. J. Heat Mass Transfer, 39 (16): 3431-3439.